



## Strength characteristics of dry and saturated rock at different strain rates

Zi-long ZHOU, Xin CAI, Yuan ZHAO, Lu CHEN, Cheng XIONG, Xi-bing LI

School of Resources and Safety Engineering, Central South University, Changsha 410083, China

Received 14 January 2016; accepted 6 June 2016

**Abstract:** The strength of rock materials is largely affected by water and loading conditions, but there are few studies on mechanical properties of saturated rocks at high strain rates. Through compressive tests on dry and saturated sandstone specimens, it was found that the dynamic compressive strength of both dry and saturated sandstone specimens increased with the increase of strain rates. The saturated rock specimens showed stronger rate dependence than the dry ones. The water affecting factor (WAF), as the ratio of the strength under dry state to that under saturated state, was introduced to describe the influence of water on the compressive strength at different strain rates. The WAF under static load was close to 1.38, and decreased with the increase of strain rate. When the strain rate reached  $190 \text{ s}^{-1}$ , the WAF reduced to 0.98. It indicates that the compressive strength of saturated specimens can be higher than that of dry ones when the strain rate is high enough. Furthermore, the dual effects of water and strain rate on the strength of rock were discussed based on sliding crack model, which provided a good explanation for the experimental results.

**Key words:** rock; strength; strain rate; saturated rock

### 1 Introduction

Water plays an important role in controlling the strength of rocks. In order to investigate the influences of water on the strength of rock material, the static compressive strength of saturated rock materials has been widely studied. COLBACK and WIID [1] showed that the uniaxial compressive strength of well-saturated quartzitic sandstone could reduce up to 50%. BROCH [2] reported the unconfined compressive strength reductions of 33%–53% for phaneritic igneous and metamorphic rocks of low porosity (0.3%–1.2%) from dry to saturated state. HAWKINS and MCCONNELL [3] investigated the influence of water content on the strength and deformability of 35 different British sandstone rocks and proposed an empirical relationship between water content and uniaxial compressive strength. VÁSÁRHELYI [4] also conducted a lot of experiments to investigate the effect of water saturation on the static properties of rocks and obtained the relationship between different petro-physical parameters. LI et al [5] accomplished a large amount of tests on two kinds of meta-sedimentary rock specimens (meta-siltstone and

meta-sandstone) under triaxial compression, and found that when the state of rock specimen changed to wet from dry, the peak cohesion increased by about 3% while the friction angle decreased by 26% for meta-siltstone; and the peak cohesion increased by about 14% while the friction angle decreased by 10% for meta-sandstone. From the above, it is commonly understood that the static compressive strength of fully saturated rock materials is usually smaller than that of dry ones.

However, all the researches mentioned above were based on static tests, limited studies can be found on the dynamic properties of saturated rocks. In fact, the rock and rock mass are usually broken and failed dynamically in rock engineering applications, such as impact, explosion, rock burst and seismic events, thus the investigation on the dynamic compressive strength weakened by water is greatly meaningful to assess the stability of rock structure and control the hazard of rock engineering. To examine the effect of water on dynamic tensile strength, OGATA et al [6] conducted a series of SHPB experiments at high porosity sandstone in both dry and saturated state and claimed that water reduced dynamic tensile strength as in the dry state. HUANG et al [7] investigated the water-weakening effect on the

tensile strength of Longyou sandstone with a wide range of loading rates, their experimental results demonstrated that the tensile strength of sandstone is water softening and the softening factor decreases with the increase of loading rate. ZHOU et al [8] carried out lots of impact tests on sandstone with different water contents, and found that when the strain rate is  $100 \text{ s}^{-1}$ , both of dynamic compressive and tensile strengths of rock decrease with the increase of water content. By now, the properties and the water-weakening mechanisms of rock under dynamic compression are not acceptable universally. Thus, more information about the effect of water on the dynamic properties of rocks at different strain rates should be investigated.

In this study, tests have been conducted on both dry and saturated sandstone specimens in a wide range of strain rates by means of the INSTRON and Split Hopkinson Pressure Bar (SHPB) setup, the strength with the same strain rate but different saturation states was compared, and the strain rate sensitivity of the compressive strength was also examined. In addition, different rate sensitivity and variation of strength of both dry and saturated sandstone specimens were explained based on the sliding crack model.

## 2 Experimental

### 2.1 Specimen preparation

The rock material was a fine-grained sandstone. The mineral composition of this sandstone was determined by X-ray diffraction (XRD). It consists of 55% quartz, 23% feldspar, 9% mica, 6% calcite, 3% chlorite and a few clay minerals (1%–4%). Some essential physical properties of the sandstone were measured as density  $2337.5 \text{ kg/m}^3$ , porosity 6.2%, and P-wave velocity  $2640.9 \text{ m/s}$ .

All specimens were extracted from a single sandstone block which had high geometrical integrity and petro-graphic uniformity. They were manufactured in accordance with the standards in the ISRM (International Society for Rock Mechanics) suggested specification [9]. The ends of specimens were polished to ensure the surface roughness less than 0.02 mm and the end surface perpendicularity to its axis less than 0.001 rad. After the measurement of the dimensions of all specimens, the P-wave velocities of all specimens were also measured to pick out specimens with similar velocity for the tests.

The static compressive tests were conducted on INSTRON system. The average static compressive strength of the dry specimens was 34.8 MPa, and that of the saturated ones was 25.5 MPa.

### 2.2 SHPB technique and its principle

SHPB is a very popular and promising experimental

technique for the study of material behaviors at different strain rates for its easy operation and accurate results [9]. As shown in Fig. 1, the SHPB system, modified by LI et al [10,11], consists of a cone-shaped striker bar, an input bar, an output bar and an absorption bar, which are made of high strength 40Cr steel with a density of  $7800 \text{ kg/m}^3$ , an elastic modulus of 250 GPa and a yield strength of 800 MPa.

During a test, the cone-shaped striker bar was shot out from the gas gun at a high velocity and impacted the front end of the input bar. Then, a half-sine wave (input wave) was generated and propagated along the input bar towards the specimen. Once the wave reached the bar/specimen interface, a part of it was reflected, whilst the remaining part went through the specimen and transmitted into the output bar. By collecting signals on the input and output bars (Fig. 1), the dynamic parameters of the specimen can be obtained.

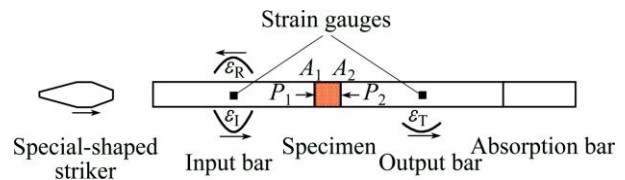


Fig. 1 Schematic of SHPB technique

In Fig. 1,  $A_1$  denotes the input bar/specimen interface and  $A_2$  represents the specimen/output bar interface.  $\varepsilon$  represents the measured signals on the bars, where the subscripts I, R and T represent incident, reflected and transmitted pulses, respectively. The arrowheads show the direction of wave propagation. According to SHPB principles, the relationship of the stress, strain and strain rate of the specimen can be derived as follows:

$$\sigma(t) = \frac{A_e E_e}{2A_s} [\varepsilon_I(t) + \varepsilon_R(t) + \varepsilon_T(t)] \quad (1)$$

$$\varepsilon(t) = \frac{C_e}{L_s} \int_0^t [\varepsilon_I(t) - \varepsilon_R(t) - \varepsilon_T(t)] dt \quad (2)$$

$$\dot{\varepsilon}(t) = \frac{C_e}{L_s} [\varepsilon_I(t) - \varepsilon_R(t) - \varepsilon_T(t)] \quad (3)$$

where  $A_e$ ,  $C_e$  and  $E_e$  are the cross sectional area ( $\text{mm}^2$ ), wave velocity (km/s) and elastic modulus of elastic bars (GPa), and  $A_s$  and  $L_s$  are the cross-sectional area ( $\text{mm}^2$ ) and length of the specimen (mm), respectively.

### 2.3 Experimental program

A total of 60 specimens were prepared in dynamic compressive tests. Firstly, specimens were placed in a  $105 \text{ }^\circ\text{C}$  oven long enough to reach the completely dry state, then the dry masses of the specimens were measured after they had cooled down to room

temperature. Then, half of them were selected and immersed into purified water within an airtight container maintained in a vacuum environment for 48 h. At that time, these specimens were considered to be completely saturated. Before tests, all prepared specimens were put into airtight plastic bags and stored in a room at constant temperature.

As known, in SHPB tests, the strain rates of specimens were mainly controlled by adjusting the gas pressure. To obtain the dynamic compressive strength of sandstone specimens with a wide range of strain rates, specimens should be impacted under different gas pressures. Before formal tests, preliminary tests were conducted to determine the range of gas pressures. During the preliminary tests, it was found that no obvious damage occurred in the sandstone specimens until the gas pressure increased to 0.4 MPa, at that time, the specimen fractured into a number of large size fragments or only macro-cracks were generated, whereas the sandstone specimens were crushed into powder when the gas pressure was adjusted to 0.7 MPa. Considering the preliminary tests results and the research objective, the range of gas pressures was determined from 0.4 to 0.8 MPa for the dynamic compressive tests. The strain rates of specimens were from 50 to 250 s<sup>-1</sup>.

The test procedures were in accordance with the ISRM suggested methods [9], and the details of parameters and results of dry and saturated specimens are shown in Tables 1 and 2, respectively.

### 3 Test results and discussion

#### 3.1 Compressive strength under different strain rates

Figure 2 shows the compressive strength of dry and saturated specimens under different strain rates. The static test results were also denoted. It can be seen that the compressive strength of saturated specimens is obviously lower than that of dry specimens under static compressive test, and the difference value decreases with the increase of strain rate. When the strain rate reaches about 180 s<sup>-1</sup>, the compressive strengths of dry and saturated specimens are close to equal. After that, the compressive strength of saturated specimens is even greater than that of dry specimens.

#### 3.2 Dynamic increasing factor

It can also be seen from Fig. 2 that the compressive strength of both the dry and saturated specimens is rate-dependent, i.e., the compressive strength increases with the increase of strain rate. The dynamic increasing factor (DIF) under different strain rates is often introduced to represent the effect of strain rate on the compressive strength of rock specimen [12,13]. The DIF is defined as

**Table 1** Parameters and test results of dry specimens in dynamic compressive tests

Specimen No.	Diameter/mm	Length/mm	P-wave velocity/(m s <sup>-1</sup> )	Strain rate/s <sup>-1</sup>	Strength/MPa
DD-1	49.09	50.04	2647.7	77	48.77
DD-2	48.92	50.05	2644.0	71	49.21
DD-3	49.05	50.02	2642.4	83	50.97
DD-4	49.03	50.00	2629.4	88	51.42
DD-5	48.93	49.98	2629.8	96	54.09
DD-6	48.98	50.01	2635.1	92	51.84
DD-7	48.91	50.00	2640.9	101	51.18
DD-8	48.98	49.99	2626.3	98	55.90
DD-9	48.93	50.01	2638.2	109	57.93
DD-10	48.96	50.03	2656.8	112	55.12
DD-11	49.06	50.01	2649.9	113	56.65
DD-12	49.06	50.06	2622.7	117	56.46
DD-13	49.00	49.97	2624.1	135	64.33
DD-14	49.04	50.05	2658.8	147	62.90
DD-15	49.03	50.06	2655.4	140	64.12
DD-16	49.00	50.08	2631.8	149	64.06
DD-17	49.03	50.08	2653.8	154	65.11
DD-18	48.99	50.06	2659.5	155	68.93
DD-19	49.07	50.00	2651.5	160	65.01
DD-20	48.98	50.06	2657.9	160	64.35
DD-21	48.93	50.02	2642.6	162	66.33
DD-22	49.04	50.03	2639.6	170	73.14
DD-23	48.93	49.96	2624.8	175	74.03
DD-24	49.06	49.96	2639.3	173	72.42
DD-25	49.00	50.02	2643.7	195	80.27
DD-26	48.96	49.92	2627.8	200	80.31
DD-27	48.96	50.03	2623.7	204	81.47
DD-28	48.91	50.06	2648.4	228	88.66
DD-29	48.98	50.02	2654.0	229	89.06
DD-30	49.02	49.98	2626.0	223	89.12

$$S_d = \frac{\tilde{\sigma}_d}{\sigma_s} \quad (4)$$

where  $S_d$  is the DIF,  $\tilde{\sigma}_d$  is the dynamic compressive strength and  $\sigma_s$  is the static compressive strength.

To quantify the rate dependency, both the dynamic compressive strengths of dry and saturated specimens at strain rates of 70, 90, 110, 130, 150, 170, 190, 210 and 230 s<sup>-1</sup> were picked out and the DIFs were calculated. As shown in Fig. 3, the compressive strength of saturated specimens has higher rate dependence than that of dry ones, and their difference is observed to increase with increasing strain rates. For example, at strain rate of 90 s<sup>-1</sup>, the DIFs of dry and saturated sandstone specimens and the difference are 1.46, 1.68 and 0.22, respectively.

**Table 2** Parameters and test results of saturated specimens in dynamic compressive tests

Specimen No.	Diameter/mm	Length/mm	P-wave velocity/(m s <sup>-1</sup> )	Strain rate/s <sup>-1</sup>	Strength/MPa
DS-1	49.03	50.06	3107.7	82	44.19
DS-2	49.01	50.04	3109.3	74	40.72
DS-3	48.97	49.94	3093.5	86	45.28
DS-4	48.97	49.98	3105.6	83	45.00
DS-5	48.94	50.05	3068.0	86	43.36
DS-6	49.03	49.95	3089.3	96	48.90
DS-7	49.01	49.91	3059.1	93	41.57
DS-8	48.96	49.98	3107.0	98	42.84
DS-9	49.00	49.92	3059.4	106	44.43
DS-10	49.02	49.96	3072.1	106	44.00
DS-11	48.96	50.06	3097.3	101	42.88
DS-12	48.92	50.09	3082.2	102	41.99
DS-13	48.93	50.04	3082.8	119	52.09
DS-14	49.00	50.00	3113.3	122	52.86
DS-15	49.02	49.94	3114.4	114	47.78
DS-16	48.96	50.05	3092.1	136	59.52
DS-17	49.08	49.95	3118.3	144	66.21
DS-18	49.05	49.95	3119.2	149	63.76
DS-19	48.93	49.95	3085.8	148	66.83
DS-20	48.98	49.98	3092.7	154	59.57
DS-21	48.98	50.05	3059.3	156	66.45
DS-22	49.05	49.92	3110.9	155	64.04
DS-23	49.01	49.97	3068.1	172	71.85
DS-24	49.03	50.05	3073.1	175	71.00
DS-25	48.93	50.01	3109.9	196	82.34
DS-26	48.97	50.03	3097.8	200	83.17
DS-27	49.02	50.07	3104.4	211	82.13
DS-28	49.02	50.03	3102.8	221	89.36
DS-29	48.97	49.94	3081.0	228	95.54
DS-30	48.93	50.09	3096.8	230	93.71

While at the strain rate of 110 s<sup>-1</sup>, they increase to 1.63, 1.98 and 0.35, respectively.

**3.3 Water affecting factor**

According to Fig. 2, at the same strain rate, the compressive strength of saturated specimen is obviously different from that of dry specimen because of water effect. To quantify this effect, the water affecting factor (WAF) is introduced. It is expressed as

$$S_w = \frac{\sigma_d}{\sigma_w} \tag{5}$$

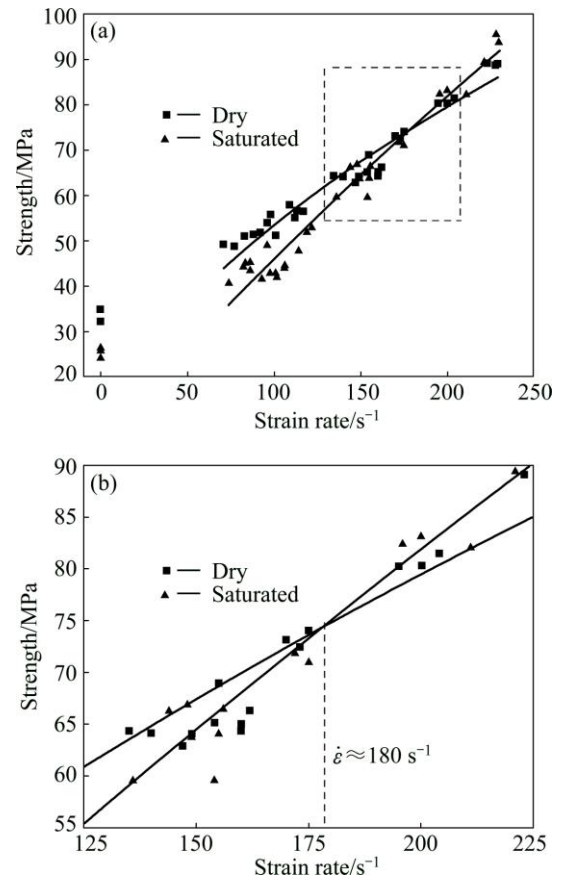


**Fig. 2** Variation of compressive strength with strain rate: (a) Test results and fitted lines; (b) Magnified view

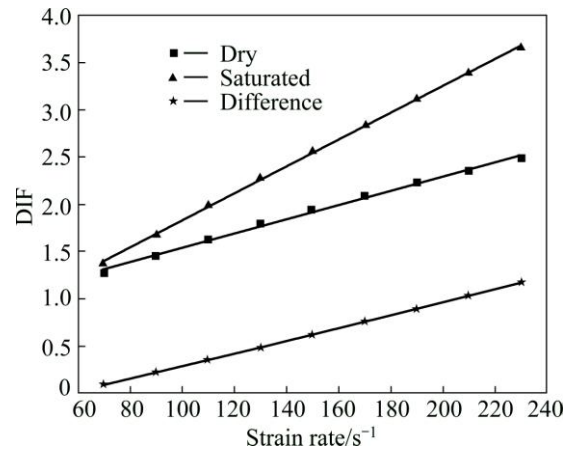


**Fig. 3** Variation of DIF with strain rate

where  $S_w$  is the WAF,  $\sigma_d$  is the compressive strength of dry specimen, and  $\sigma_w$  is the compressive strength of saturated specimen.

Figure 4 shows the WAF at different strain rates. It can be seen that the WAF obviously decreases with the increase of strain rate, which indicates that the water may have stronger effect on dynamic compressive strength under higher strain rates. Particularly, when the strain rate reaches 190 s<sup>-1</sup>, the WAF is approximately 0.98, i.e.,

the compressive strength of saturated specimens is even higher than that of dry ones at that time.

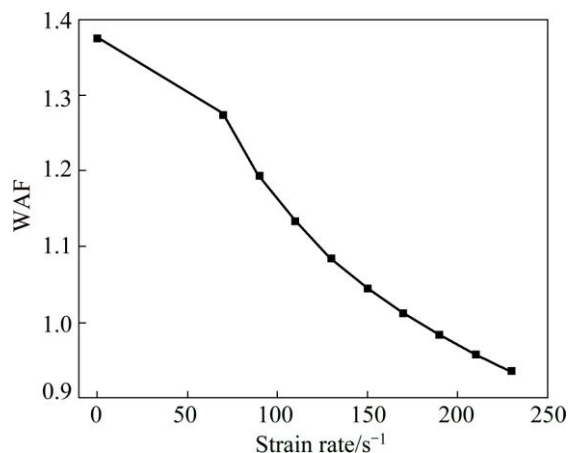


Fig. 4 Variation of WAF with strain rate

## 4 Micro-mechanics analysis based on sliding crack model

In recent years, researchers have studied the mechanical properties of rock materials under compressive loads by analyzing the initiation and propagation of cracks, and proposed several micro-mechanics models. Among them, the sliding crack model is widely accepted, which considered that the failure of rock materials is controlled by the initiation and propagation of micro cracks [14–16].

### 4.1 Mechanism of water decreasing strength of saturated rock in static compressive tests

In static tests, it is found that the compressive strength of the saturated rocks is lower than that of the dry ones. For saturated specimens, several chemical and physical reactions might happen between free water and minerals, which weaken the connection between mineral particles, thereby reducing the overall strength and elastic modulus of rocks.

In addition, free water has lubricating effect on initial cracks. This would decrease the friction between the initial crack surfaces, and further promotes the slide of initial crack and creation of tensile cracks.

Besides, when the rock is under static compressive condition, the free water in the specimen can arrive at the crack tips because of the slow crack propagation speed. In the presence of external pressure, free water inside the rock results in porous water pressure, also called crack splitting tensile stress ( $P_1$ ), which further promotes the crack propagation like water wedges into cracks, thereby reducing the compressive strength of rock (Fig. 5(a)). All of these could explain the rock strength reduction due to the increase of water content under the static compressive condition.

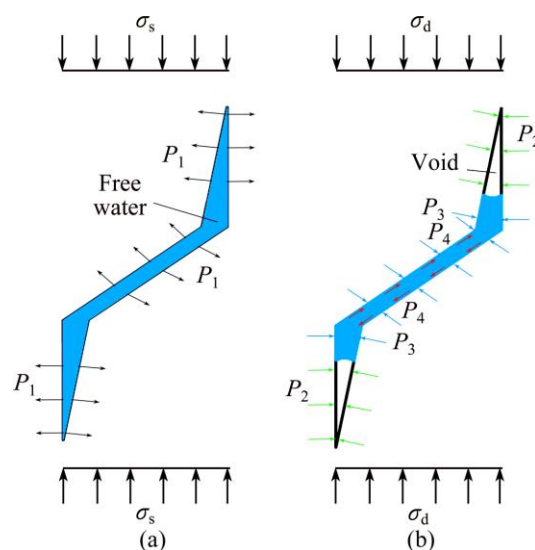


Fig. 5 Stress induced by water in static compressive test (a) and in dynamic compressive test (b)

### 4.2 Mechanism of water increasing strength of saturated rock in dynamic compressive tests

In static tests, water can weaken the compressive strength of rock. However, when rock fails under high strain rate condition, the viscous behavior of water, including the meniscus effect, the Stefan effect and the Newton inner friction law, can delay the creation and propagation of tensile cracks, thus exerting positive influence on dynamic compressive strength of rocks.

#### 4.2.1 Meniscus effect

During the dynamic compressive tests, the cracks expand very fast which could even reach 1000 m/s [17], and consequently free water fails to get to the crack tips timely. So the splitting effect of water ( $P_1$ ) does not work on the cracks. At the same time, free water in the cracks would form a meniscus which can cause resisting stress to the propagation of cracks (Fig. 5(b)). That is called meniscus effect [18,19] and the resisting stress ( $P_2$ ) of meniscus effect can be expressed by

$$P_2 = \frac{2\gamma_w \cos \alpha}{\rho} \quad (6)$$

where  $P_2$  is the resisting stress of the meniscus effect,  $\gamma_w$  is the surface energy of water,  $\alpha$  is the wetting angle, and  $\rho$  is the radius of curvature of meniscus.

#### 4.2.2 Stefan effect

As shown in Fig. 6, there are two parallel circular plates, the thin space between the two plates is filled with an incompressible liquid (e.g. water or oil). When the two plates are taken apart at a relative velocity in the vertical direction, the liquid will exert a resisting stress on the two plates. This physical phenomenon is called Stefan effect. The resisting stress can be expressed by [20]

$$P_3 = \frac{3\eta R^2}{2h^3} \cdot \dot{h} \quad (7)$$

where  $P_3$  is the resisting stress of the Stefan effect,  $\eta$  is the viscosity of water,  $R$  is the radius of the plates,  $h$  is the initial distance between the two plates and  $\dot{h}=dh/dt$  is the relative velocity of the two plates.

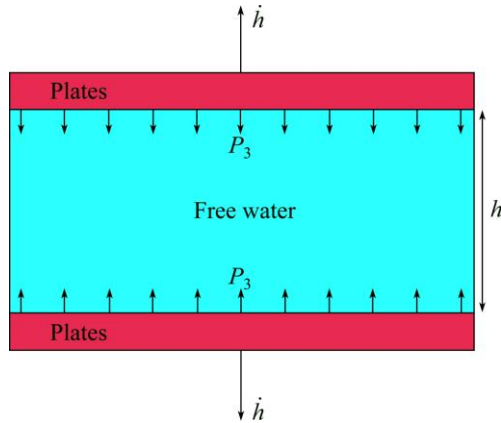


**Fig. 6** Resisting stress induced by Stefan effect between two plates

Here we attempt to combine the Stefan effect with the crack propagation of rock. The solid skeletons of rock materials can be regarded as many plates, and the free water in pores is incompressible liquid between the plates.  $dh$  is considered as the relative displacement of crack, and it is proportional to external stress  $\sigma$  according to the linear fracture mechanics [7]. Besides, the loading rate ( $\dot{\sigma}$ ) and strain rate ( $\dot{\epsilon}$ ) are equivalent for the dynamic test [9], thus

$$P_3 \propto \frac{dh}{dt} \propto \dot{\sigma} \propto \dot{\epsilon} \quad (8)$$

It can be seen from Eq. (8) that, the resisting stress of the Stefan effect is proportional to the strain rate of rock. For the saturated rocks under dynamic tests, the higher the strain rate is, the higher the induced resisting stress will be. It explains the rate dependence of saturated rocks under higher strain rates very well.

#### 4.2.3 Newton inner friction effect

As illustrated in Fig. 7, there are two parallel plates with water filled between them. The two plates are big enough to neglect the edge effect. When the upper plate is forced to move parallel to the bottom one with a relative velocity  $u$ , the water will exert the resisting stress. This is called Newton inner friction effect [21]. According to Newton’s equation of viscosity, the inner friction between water and rock ( $P_4$ ) can be expressed by

$$P_4 = \eta \frac{du}{dy} \quad (9)$$

where  $\eta$  is the viscosity of water,  $u$  is the relative sliding

velocity, and  $du/dy$  is the velocity gradient.

According to the linear fracture mechanics, the relative sliding displacement ( $udt$ ) of initial crack is proportional to the external stress  $\sigma$ , thus

$$P_4 \propto \frac{du}{dy} \propto \dot{\sigma} \propto \dot{\epsilon} \quad (10)$$

It can be seen from Eq. (10) that, the inner friction between water and plate is proportional to sliding velocity of the plate. As mentioned above, the micro-cracks in the rock can be treated as the plates. In the dynamic tests, the higher the strain rate is, the quicker the crack (plate) moves. So, the induced inner friction between water and micro-cracks will be higher. In static tests, the influence of inner friction stress is much smaller, therefore, the Newton inner friction law can be neglected.

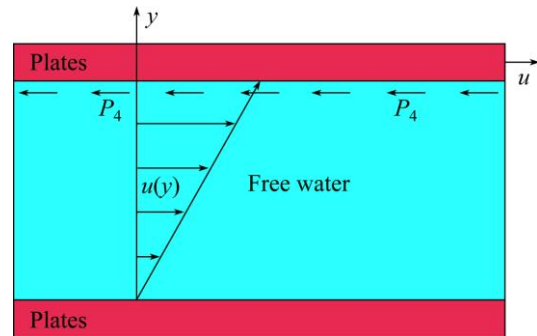


**Fig. 7** Resisting stress induced by Newton inner friction effect between two plates

In summary, the rate dependence of saturated specimens is caused by both the rock skeleton and viscous behaviors of free water in the pore (i.e.,  $P_3$  in Fig. 6 and  $P_4$  in Fig. 7). It is remarkable that the compressive strength of saturated specimen is still lower than that of dry specimen at lower strain rate. Only when the strain rate is high enough, the meniscus effect, Stefan effect and Newton inner friction effect can be obvious. When the water weakening effect on rock skeleton is completely offset by the increasing viscous stress of water, the compressive strength of saturated specimens becomes higher than that of dry specimens.

## 5 Conclusions

1) The compressive strength of both the dry and saturated sandstone specimens is rate-dependent, and the compressive strength of saturated specimens shows higher rate dependence than that of dry ones.

2) The compressive strength of saturated specimens is lower than that of dry ones in static tests, however, when the strain rate exceeds  $180 \text{ s}^{-1}$  in dynamic tests, the compressive strength of saturated specimens will be

higher than that of dry specimens.

3) In static tests, water weakens the rock skeleton and the overall strength. In dynamic tests, viscous stress of water for the meniscus effect, Stefan effect and Newton inner friction effect can increase the overall strength greatly.

## References

- [1] COLBACK P, WIID B L. The influence of moisture content on the compressive strength of rocks [C]//Proceedings of the 3rd Canadian Rock Mechanism Symposium, 1965: 65–83.
- [2] BROCH E. The influence of water on some rock properties [C]//Proceedings of the 3rd Congress ISRM. 1974: 33–38.
- [3] HAWKINS A B, MCCONNELL B J. Sensitivity of sandstone strength and deformability to changes in moisture content [J]. Quarterly Journal of Engineering Geology and Hydrogeology, 1992, 25(2): 115–130.
- [4] VÁSÁRHELYI B. Statistical analysis of the influence of water content on the strength of the Miocene limestone [J]. Rock Mechanics and Rock Engineering, 2005, 38(1): 69–76.
- [5] LI D, WONG L N Y, LIU G, ZHANG X. Influence of water content and anisotropy on the strength and deformability of low porosity meta-sedimentary rocks under triaxial compression [J]. Engineering Geology, 2012, 126: 46–66.
- [6] OGATA Y, JUNG W, KUBOTA S, WADA Y. Effect of the strain rate and water saturation for the dynamic tensile strength of rocks [J]. Materials Science Forum, 2004, 465: 361–366.
- [7] HUANG S, XIA K, YAN F, FENG X. An experimental study of the rate dependence of tensile strength softening of Longyou sandstone [J]. Rock Mechanics and Rock Engineering, 2010, 43(6): 677–683.
- [8] ZHOU Z L, CAI X, CAO W Z, LI X B, XIANG C. Influence of water content on mechanical properties of rock in both saturation and drying processes [J]. Rock Mechanics and Rock Engineering, 2016: 10.1007/s00603-016-0987-z.
- [9] ZHOU Y X, XIA K, LI X B, LI H B, MA G W, ZHAO J, ZHOU Z L, DAI F. Suggested methods for determining the dynamic strength parameters and mode-I fracture toughness of rock materials [M]//The ISRM Suggested Methods for Rock Characterization, Testing and Monitoring: 2007-2014. Springer International Publishing, 2011: 35–44.
- [10] LI X B, ZHOU Z L, LIU D S, ZOU Y, YIN T B. Wave shaping by special shaped striker in SHPB tests [M]//Advances in Rock Dynamics and Applications. Boca Raton: CRC Press, 2011: 105–123.
- [11] ZHOU Z L, LI X B, LIU A H, ZOU Y. Stress uniformity of split Hopkinson pressure bar under half-sine wave loads [J]. International Journal of Rock Mechanics and Mining Sciences, 2011, 48(4): 697–701.
- [12] ZHANG Q B, ZHAO J. A review of dynamic experimental techniques and mechanical behaviour of rock materials [J]. Rock Mechanics and Rock Engineering, 2014, 47(4): 1411–1478.
- [13] XIA K, YAO W. Dynamic rock tests using split Hopkinson (Kolsky) bar system — A review [J]. Journal of Rock Mechanics and Geotechnical Engineering, 2015, 7(1): 27–59.
- [14] LI H B, ZHAO J, LI T J. Micromechanical modelling of the mechanical properties of a granite under dynamic uniaxial compressive loads [J]. International Journal of Rock Mechanics and Mining Sciences, 2000, 37(6): 923–935.
- [15] BRACE W F, BOMBOLAKIS E G. A note on brittle crack growth in compression [J]. Journal of Geophysical Research Atmospheres, 1963, 68(12): 3709–3713.
- [16] HORII H, NEMAT-NASSER S. Brittle failure in compression: splitting, faulting and brittle-ductile transition [J]. Philosophical Transactions of the Royal Society of London A: Mathematical, Physical and Engineering Sciences, 1986, 319(1549): 337–374.
- [17] ZHANG Q B, ZHAO J. Effect of loading rate on fracture toughness and failure micromechanisms in marble [J]. Engineering Fracture Mechanics, 2013, 102(2): 288–309.
- [18] ROSSI P. A physical phenomenon which can explain the mechanical behaviour of concrete under high strain rates [J]. Materials & Structures, 1991, 24(24): 422–424.
- [19] WANG H, JIN W, LI Q, LI Q B. Saturation effect on dynamic tensile and compressive strength of concrete [J]. Advances in Structural Engineering, 2009, 12(2): 279–286.
- [20] ZHENG D, LI Q. An explanation for rate effect of concrete strength based on fracture toughness including free water viscosity [J]. Engineering Fracture Mechanics, 2004, 71(16–17): 2319–2327.
- [21] FRANZINI J B. Fluid mechanics with engineering applications [M]. Tata McGraw-Hill Education, 1975.

## 不同应变率下干、湿岩石的强度特性

周子龙, 蔡鑫, 赵源, 陈璐, 熊成, 李夕兵

中南大学 资源与安全工程学院, 长沙 410083

**摘要:** 水和加载条件对岩石材料的强度有很大的影响, 但高应变率下饱水岩石的动态特性研究仍十分缺乏。通过对干燥和饱水砂岩进行压缩试验, 发现: 干燥和饱水砂岩的动态压缩强度都随着应变率的增加而增大, 且饱水岩石表现出更强的率相关性。引入干燥岩石强度与饱水岩石强度的比值(水影响因子 WAF)来描述不同应变率下水对岩石压缩强度的影响。在静态压缩条件下 WAF 约为 1.38, 随着应变率的增加 WAF 不断减小。当应变率达到  $190 \text{ s}^{-1}$  时, WAF 减小至 0.98, 表明高应力率时饱水岩石的压缩强度可以大于干燥岩石的压缩强度。进而, 基于滑移裂纹模型, 讨论了水和应变率对岩石特性的双重影响, 为实验结果提供了较好解释。

**关键词:** 岩石; 强度; 应变率; 饱水岩石

(Edited by Sai-qian YUAN)